IEEE Access
Multidisciplinary : Rapid Review : Open Access Journal

Received February 7, 2018, accepted March 12, 2018, date of publication March 16, 2018, date of current version April 23, 2018.

Digital Object Identifier 10.1109/ACCESS.2018.2816684

Remaining Useful Life Prediction for Lithium-Ion Batteries Based on Exponential Model and Particle Filter

LIJUN ZHANG[1], ZHONGQIANG MU[1], AND CHANGYAN SUN[2]
[1]National Center for Materials Service Safety, University of Science and Technology Beijing, Beijing 100083, China
[2]School of Chemistry and Biological Engineering, University of Science and Technology Beijing, Beijing 100083, China

Corresponding author: Lijun Zhang (ljzhang@ustb.edu.cn)

This work was supported in part by the National Key Research and Development Program of China under Grant 2016YFF0203804, in part by the National Natural Science Foundation of China under Grant 51775037, and in part by the Fundamental Research Funds for Central Universities of China under Grant FRF-TP-15-010A3.

ABSTRACT As the secondary widely used battery, lithium-ion batteries (LIBs) have become the core component of the energy supply for most devices. Accurately predicting the current cycle time of LIBs is of great importance to ensure the reliability and safety of the equipment. In this paper, considering the nonlinear and non-Gaussian capacity degradation characteristics of LIBs, a remaining useful life (RUL) prediction method based on the exponential model and the particle filter is proposed. The cycle life test data of LIBs published by prognostics center of excellence in national aeronautics and space administration were exponentially experiencing the rule of degradation. And then the extrapolation method was used to get the quantitative expression of the uncertainty of life expectancy of LIBs, i.e. the prediction mean and the probability distribution histogram. The prognostic horizon index and the new specific accuracy index were applied to evaluate the prediction performance. Moreover, the prediction error under different prediction starting points is given. Compared with other methods such as the auto-regressive integrated moving average model, the fusion nonlinear degradation autoregressive model and the regularized particle filter algorithm, the proposed algorithm has a better prediction performance. According to the accuracy index, the proposed prediction method has better prediction accuracy and convergence. The RUL prediction for LIBs can provide a better decision support for the maintenance and support systems to optimize maintenance strategies, and reduce maintenance costs.

INDEX TERMS Lithium-ion batteries (LIBs), exponential model, particle filter (PF), remaining useful life (RUL) prediction.

I. INTRODUCTION

Lithium-ion batteries (LIBs) have been widely used in electric vehicles because of its energy density, small weight, long life, and no memory effect [1]–[4]. However, due to operating conditions and the impact of aging, the performance of LIBs will degrade and lead to failure [5]; some security incidents and even catastrophic accidents will occur in the event of failure because of a large energy density [6], [7]. For many applications of LIBs in the fully charged state, the end of life of LIBs can be defined as the point when the actual capacity declined 70$\sim$80% of the nominal capacity or the actual internal resistance increased to 1.6$\sim$2 times of the initial internal resistance [8].

A remaining useful life (RUL) prediction is critical to the implementation of condition based maintenance (CBM) and prognostics and health management (PHM) [9]. In recent years, in order to make the system of LIBs operation more reliable and safe, the battery management system (BMS) with independent health management function has become the direction for future research and development [10]. So it is important to find a reliable and accurate method to predict RUL to provide maintenance and replacement of the BMS in a timely manner [11], [12].

Now, scholars have carried out extensive efforts on the research of RUL prediction methods for LIBs. Zhang, *et al.* [13] focused on a battery capacity prognostic approach using the empirical mode decomposition (EMD) denoising method and the multiple kernel relevance vector machine (MKRVM) approach, and the proposed MKRVM approach can predict the battery's future capacity precisely. Andre, *et al.* [14] proposed a priori knowledge-based structured neural network (SNN) method, and established voltage, current and impedance of the mathematical expression according to the equivalent circuit model of LIBs. The ensemble monotonic echo state networks (En_MONESN) algorithm [15] and the Gaussian process regression (GPR) algorithm [16] were proposed for RUL of LIBs. Long, *et al.* [17] used the autoregressive (AR) model to track the degradation trend of the capacity of LIBs, and then used the particle swarm optimization algorithm to determine the order of the AR model for achieving the RUL prediction of LIBs. In Zhou's research [18], the capacity degradation process of LIBs is regarded as a multi-component mixed signal. The support vector machine (SVM) algorithm [19], [20] was introduced to LIBs. Wang, *et al.* [11] and Liu, *et al.* [21] estimated the capacity of LIBs using a relevance vector machine (RVM) algorithm and a conditional three-parameter capacity degradation model. Peng, *et al.* [22] proposed a method based on the adaptive unscented Kalman filter (AUKF) with a noise statistics estimator to estimate accurately state of charge (SOC) of battery energy storage systems, and the proposed method can achieve the better SOC estimation accuracy when the noise statistics of battery energy storage systems are unknown or inaccurate. And there are also some fusion methods on state-of-health prediction and management of LIBs in the literature [23]–[25].

A particle filter (PF) is a typical used method to determine the RUL uncertainty of LIBs. From the literature, the life expectancy of the PF has a very good prospect because of its strong nonlinear, non-Gaussian processing capacity [26]. But the PF itself has two main problems: particle degradation and sample deprivation [27]. Although resampling can reduce particle degradation to a certain extent, it can also lead to a lack of sample particles. Miao, *et al.* [28] used the unscented PF and Wang, *et al.* [29] used the sphere cubes PF on tackling the disadvantages about lack of sample particles. Based on the Markov Chain Monte Carlo (MCMC) algorithm, the unscented PF has been improved to enhance the diversity of particles in the process of resampling [30], [31].

However, the prediction accuracy based on the PF is controlled by the influence of the shortcomings of the algorithm itself, and in addition, it still depends on the state space model of the degradation process of LIBs. Based on the characteristics of capacity degradation of LIBs, Yang, *et al.* [32] proposed a fusion model of exponential and polynomials, and then the PF algorithm is used to update the model parameters online. Based on the characteristics of the capacity degradation of Li(NiMnCo)O_2 LIBs, Wang, *et al.* [33] proposed a double logarithmic degradation model, and then the PF algorithm was used to study the parameters. Gustafsson [34] proposed a novel incremental capacity analysis (ICA) method for state of health (SOH) estimation to optimize the model parameters for better prediction accuracy and enhance its applicability in realistic BMS, and the effectiveness of the proposed model was validated by experimentation. In this paper, the RUL prediction for LIBs based on the exponential model and the PF will be future researched.

This paper is structured as follows: Section II studies the theoretical derivation of the PF method in life prediction. The capacity degradation state space model of LIBs is established in Section III. In section IV, the prediction method based on the PF and the exponential degeneration model is studied. And experimental data of the capacity degradation of LIBs, which were published by Prognostics Center of Excellence (PCoE) in National Aeronautics and Space Administration (NASA), are analyzed to verify the validity and reliability of the proposed algorithm. Section V gives a more reasonable evaluation of the prediction performance. Finally, Section VI concludes the paper.

II. BASIC PRINCIPLE OF PARTICLE FILTER METHOD

As a machine learning algorithm, the PF has a strong ability to deal with nonlinear and non-Gaussian problems and has been widely used in various fields [11], [35]–[37]. Therefore, the research on the PF in life prediction applications has important theoretical and practical significance.

A. PARTICLE FILTER

The PF is a general algorithm based on the Bayesian estimation, which uses the Monte Carlo method to draw particles from a posterior distribution and assigns a weight to each particle [37].

The implementation of the PF algorithm [26], [35], [38] consists of the following three steps, as shown in Fig. 1. First, the algorithm generates an initial particle division, and then updates the weight of each particle, and finally re-samples in accordance with the requirements.

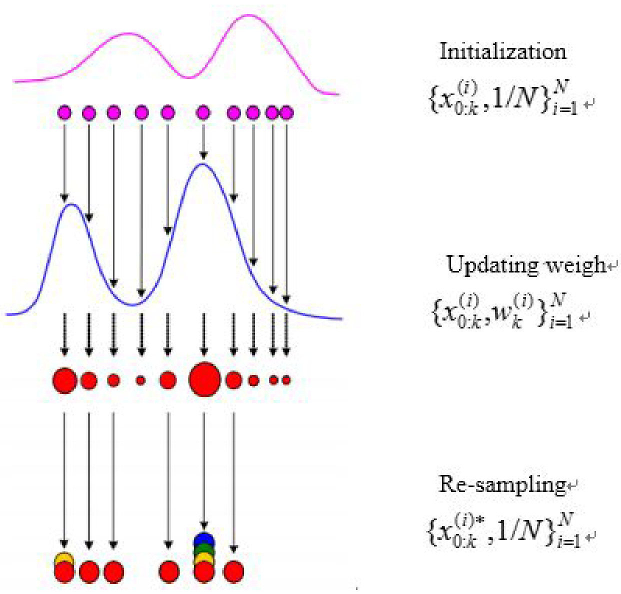

FIGURE 1. The PF implementation scheme.

(1) Initializing ($k = 0$): the generation of particles. The weight of all particles is assigned as $\tilde{w}_0^{(i)} = 1/N$, and a priori

probability density function $P(x_0)$ generates a set of sampled particles $\{x_0^{(i)}\}_{i=1}^N$.

(2) Updating the weight at the time k:

$$w_k^{(i)} = w_{k-1}^{(i)} \frac{p\left(z_k|x_k^{(i)}\right) p(x_k^{(i)}|x_{k-1}^{(i)})}{q\left(x_k^{(i)}|x_{k-1}^{(i)}, z_{1:k}\right)} \tag{1}$$

Normalizing particle weights:

$$\tilde{w}_k^{(i)} = \frac{w_k^{(i)}}{\sum_{j=1}^{N} w_k^{(j)}} \tag{2}$$

(3) Re-sampling: Calculating the number of valid samples:

$$\hat{N}_{eff} = \frac{1}{\sum_{i=1}^{N} (w_t^{(i)})^2} \tag{3}$$

If $\left\{x_{0:k}^{(i)}, w_k^{(i)}\right\}_{i=1}^{N}$, the algorithm re-samples are according to the importance weights to obtain a new set of particles $\{x_k^{(i)}, 1/N\}$; otherwise, no resampling.

State estimation:

$$\hat{x}_k = \sum_{i=1}^{N} x_k^{(i)} w_k^{(i)} \tag{4}$$

$$\hat{P}_k = \sum_{i=1}^{N} w_k^{(i)} (x_k^{(i)} - \hat{x}_k)(x_k^{(i)} - \hat{x}_k)^T \tag{5}$$

B. SPACE MODEL OF DYNAMIC SYSTEM STATE

Using a suitable model to describe a real problem is important for analyzing and solving the problem [27]. The state space model is such a very important analytical model that most of the problems can be described in many practical engineering applications such as signal processing, statistics and communications radar sonar. Specifically, the construction of a dynamic spatial model is mainly expressed by two equations as following:

$$x_k = f(x_{k-1}, \theta_k, v_k) \tag{6}$$

$$z_k = h(x_k, w_k) \tag{7}$$

where: $k = 1, 2, 3\ldots$represents a discrete time series; x_k represents the system state variable or parameter at time k; f represents the state transfer function of the system; w_k represents the process noise sequence; z_k represents the measurement of the system at time k; h represents the observation function of the system; v_k represents the measurement noise sequence.

Equation (6) describes a dynamic process in which the state of a system evolves over time, and it is therefore commonly referred to as a state transition equation which represents the system according to the Markov process with the dynamic evolution at time k. Equation (7) describes state-dependent noise variables, also is called measurement equations.

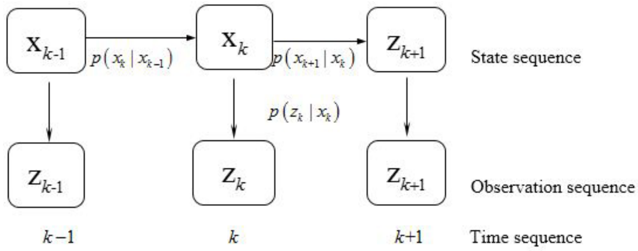

FIGURE 2. The model diagram of the dynamic system space.

The model diagram of the dynamic system space is shown as Fig. 2.

It supposes that transfer equation x_k follows the first-order Markov process and is independent of the measured value z_k, and the initial probability density function $p(x_0)$ of the state x_k is known as a priori knowledge. Then the statistical description of the dynamic system state of space model is as following.

Corresponding to the state transition model, the state transition probability density of the system is $p(x_k|x_{k-1})$. Corresponding to the observation model, the observation probability density of the system states is $p(z_k|x_k)$.

III. ALGORITHM FLOW AND DEGRADATION MODELING

In this section, the model of the capacity degradation of LIBs is established. The PF algorithm is used to study the model parameters nonlinearly, and then the probability distribution of the model parameters is obtained. The probability density distribution of the life prediction can be given by an extrapolation method with counting the life value of each particle.

A. FRAMEWORK AND ALGORITHM FLOW OF REMAINING LIFE PREDICTION OF LITHIUM-ION BATTERIES

In this paper, the PF algorithm selects the priori probability density function as an important density function, that is:

$$q\left(x_k^{(i)}|x_{k-1}^{(i)}, z_{1:k}\right) = p(x_k^{(i)}|x_{k-1}^{(i)}) \tag{8}$$

The importance weight is simplified calculated as follows:

$$w_k^{(i)} = w_{k-1}^{(i)} \frac{p\left(z_k|x_k^{(i)}\right) p(x_k^{(i)}|x_{k-1}^{(i)})}{q\left(x_k^{(i)}|x_{k-1}^{(i)}, z_{1:k}\right)} = w_{k-1}^{(i)} p\left(z_k|x_k^{(i)}\right) \tag{9}$$

The framework of the PF algorithm consists of four parts: the data preprocessing, the model parameter determination, the capacity status prediction, and the cycle life calculation. There are some parameters: b is defined as the unknown parameter of the empirical model in the capacity degradation of LIBs, T is defined as the starting point in the algorithm implementation, N is defined as the number of particles, s is defined as the standard deviation of the measured noise, U is defined as the capacity threshold at the end of the battery life, z is defined as the real value of the capacity degradation of LIBs, x is defined as the capacity prediction output value in the each step iterative process, and *cycle* is defined as the charge and discharge cycle number. The detailed steps of the algorithm are given as below.

(1) Extracting the battery capacity data z from the NASA PCoE battery test data, preprocessing the data, such as data reduction and remove outliers.

(2) Setting the predicted starting point T. The data before the starting point T are defined as the known historical data, and used as the training data parameters to update model parameters.

(3) Initializing the PF algorithm to set some parameters in the life prediction process: N, x, s, b, U.

(4) Using the PF algorithm to track the battery capacity data before the starting point T, updating the state parameters x, b and s in the degradation process of LIBs. The flow of the training algorithm is as follows:

Step 1: Initializing the particle set: $k = 0$, getting particle set $\{x_0^{(i)}\}_{i=1}^N$ and weight $\tilde{w}_0^{(i)} = 1/N$;

Step 2: Updating weight $w_k^{(i)} = w_{k-1}^{(i)} p\left(z_k|x_k^{(i)}\right)$, normalizing weight $\tilde{w}_k^{(i)}$;

Step 3: Performing resample to obtain a new particle set after resampling $\{x_{0:k}^{(i)*}, w_k^{(i)}, \}_{i=1}^N$;

Step 4: Outputting the battery capacity $\hat{C}_k = \sum_{i=1}^{N} x_k^{(i)} \tilde{w}_k^{(i)}$;

Step 5: Repeating the above steps in sequence at $k = k+1$ until $k = T$, that is, all training data are used up.

(5) Achieving the purpose of prediction: $k = T + 1$. According to the state transition function, x of each particle is iterated and it is determined whether or not x reaches U. If all are not reached, the unimplemented particles are extrapolated until all particles are reached.

(6) Calculating the RUL of each particle and doing statistical analysis to obtain the RUL distribution histogram of LIBs if all particles reach the threshold and end iteration.

In summary, Fig. 3 shows the flow chart of the algorithm that describes the method of RUL prediction for LIBs based on the exponential model and the PF.

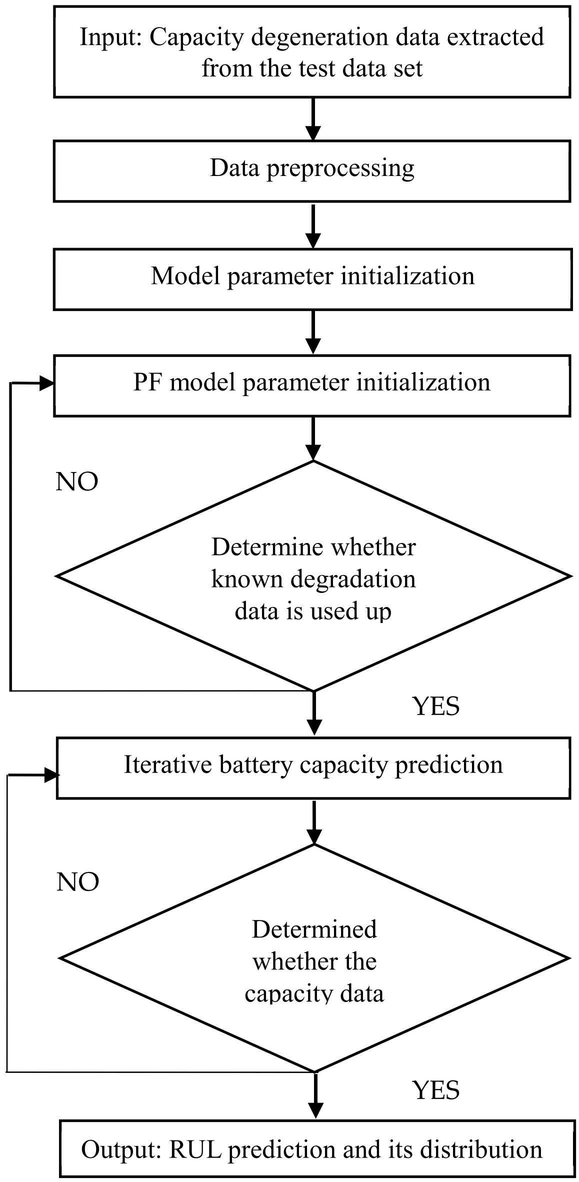

FIGURE 3. **The RUL algorithm flow chart based on the exponential model and the PF.**

B. LITHIUM-ION BATTERY CYCLE LIFE DEGRADATION MODELING

According to the PF algorithm, a state transition matrix or function of the capacity degradation of LIBs is established. In this paper, based on the experience fitting method, the mathematical relationship model between the number of cycles and the capacity is established, and then the residual life is predicted by the PF algorithm.

According to the PF algorithm and the empirical degradation model of LIBs, the degradation process can be represented by the following state space model:

$$x_k = f(x_{k-1}, \theta, w_k) = \exp(-b_k \Delta t) x_{k-1} + w_k \quad (10)$$

$$Q_k = x_k + v_k \quad (11)$$

According to the Monte Carlo integral algorithm, the posterior probability density function can be approximated by N sampling values, so the capacity Q can be calculated by the following equation:

$$Q_k \approx \sum_{i=1}^{N} w_k^{(i)} \delta(x_k - x_k^{(i)}) \quad (12)$$

where $\delta(\cdot)$ represents the Dirac Delta function, $w_k^{(i)}$ represents the particle weight.

When the number of cycle is k, the p-step prediction results of each particle can be calculated by the following equation:

$$Q_{k+p}^{(i)} = Q_k^{(i)} \exp(-b_k p) \quad (13)$$

When the capacity of LIBs dropped to 70% of the initial rated capacity, its life reaches the end value. So, the number of charge and discharge cycles can be calculated by the following equation:

$$0.7Q_{\text{rated}} = Q_k^{(i)} \exp(-b_k l_k^{(i)}) \tag{14}$$

If the initial capacity of the battery and the previous k-cycle capacity data $(Q_1, Q_2, \ldots, Q_k)$ are known, the model of the PF is used to study the model parameters, the probability density and distribution function after the p-step prediction for the capacity of LIBs can be calculated by the following equation:

$$p(l_p|Q_{0:k}) \approx \sum_{i=1}^{N} w_k^{(i)} \delta(l_{k+p} - l_{k+p}^{(i)}) \tag{15}$$

IV. REMAINING USEFUL LIFE PREDICTION FOR LITHIUM-ION BATTERIES

Combining with the capacity degradation of the actual characteristics, this section focuses on the cycle life prediction method of LIBs. A large number of case studies and experimental data set on the capacity degradation which was published by the NASA PCoE were analyzed in order to verify the effectiveness and reliability of the proposed algorithm.

A. DATA SET OF BATTERIES DEGRADATION

The experimental data set [38], which is published by PCoE in NASA, is based on the battery specification for commercial 18650.

Through the initial analysis on the battery capacity degradation data and experimental conditions, Battery005, Battery006 and Battery018 are selected to verify the effectiveness of the proposed algorithm based on the exponential model and the PF.

As these three batteries of its nominal rated capacity of 2 Ah (only slightly different cycle discharge conditions), and the failure criteria of capacity is 0.7 times the initial rated, so the life termination point of the capacity threshold is set to $U = 1.4$ Ah.

The experimental conditions of batteries cycle life are described below:

Step 1, charging with the constant current 1.5 A, changing charge model with constant voltage when the charge limit voltage reaches 4.2 V, and then stopping charging when the current is reduced to 20 mA, at last, standing time indefinite;

Step 2, discharging with constant current 2 A, stopping discharging when the voltage drops 2.7 V or 2.5 V, and at last, standing time indefinite;

Step 3, repeating the above steps, getting the data from the cycle performance degradation of LIBs.

Three single batteries were subjected to a general degradation performance test at room temperature. The capacity degradation curve was shown in Fig. 4 during the whole experiment.

As shown in Fig. 5, the nonlinear least squares method is used to exponentially quantify the capacity degradation data of LIBs. It can be seen from Fig. 5, the index model in the overall can be better to fit the data about the capacity degradation, the overall trend of the capacity attenuation can be better to basically response the rules.

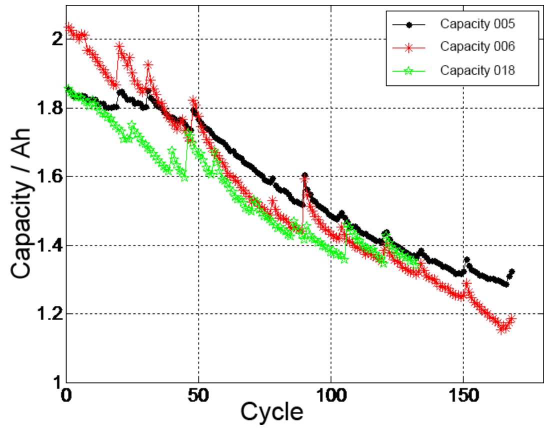

FIGURE 4. The capacity degradation curves.

If Q is used to represent the capacity of LIBs during degradation, the empirical model of its degradation can be written as:

$$Q = a \cdot \exp(-b \cdot k) \tag{16}$$

where a and b represent the model parameters and k represents the number of charge and discharge cycles.

B. UNCERTAINTY QUANTITATIVE EXPRESSION OF BATTERY CYCLE LIFE PREDICTION RESULTS

Taking the Battery005 as an example, this section illustrates how to use the algorithm proposed in this paper to predict the cycle life of LIBs.

Experimental data of Battery005 have a total 168 cycle life sample points. In order to obtain better prediction effect, the number of cycles representing the end of life is chosen as the starting point of prediction, that is, $T = 100$, and the PF with nonlinear and non-Gaussian learning ability is used to track the training for the first 100 samples. After the final parameter value of the exponential prediction model is obtained, the life expectancy prediction is achieved by the extrapolation method, and the life probability of each particle is calculated to give the predicted life probability density distribution.

In the example of Battery005, setting some necessary parameters for the algorithm to run and initialize: the number of particles $N = 5000$, through a large number of experiments to determine the optimal parameters of the value range is: the initial value of the state $x \sim U(1.7, 2.1)$, $B \sim U(0, 0.02)$, $s \sim U(0.01, 0.1)$.

After the initialization is complete, running the PF algorithm to update the state initial value: starting from $T = 100$, the parameter values of the battery are updated according to the updated state value and the state transition equation, and each particle is subjected to the iterative extrapolation.

At the same time, it is judged whether or not the capacity state value x of each particle reaches the set capacity threshold. If each particle reaches a preset capacity threshold, the recursive iteration process is ended, and the cycle life

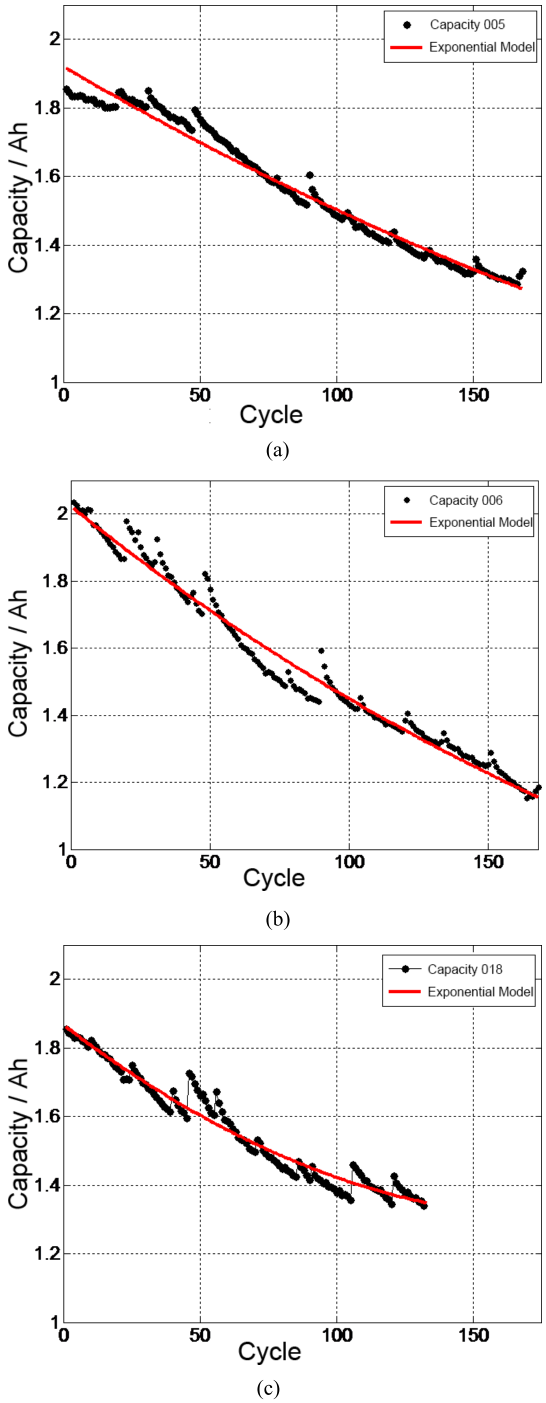

FIGURE 5. The capacity degeneration curves and its exponential fitting curves. (a) Battery005. (b) Battery006. (c) Battery018.

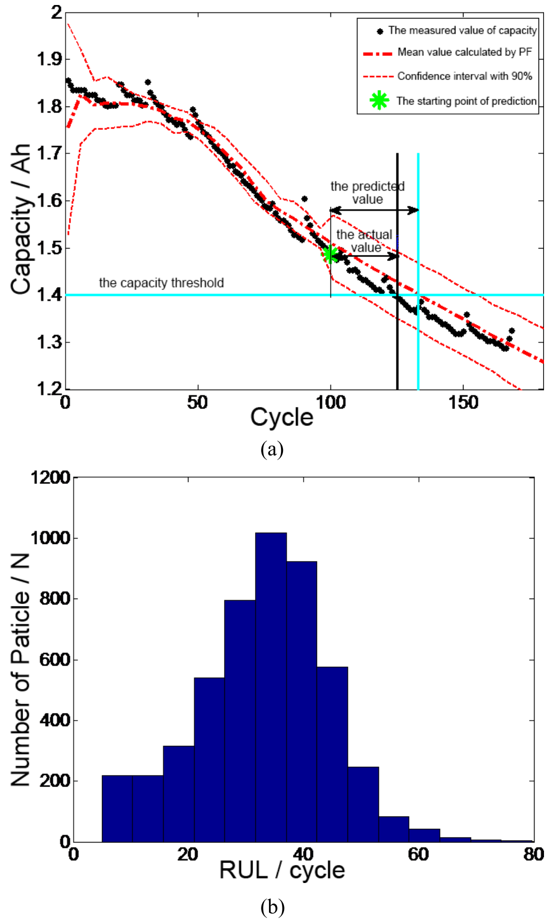

FIGURE 6. The RUL prediction results of Battery005 at the starting point $T = 100$. (a) The capacity degeneration curve. (b) The RUL distribution histogram.

value of each particle is output according to the difference between the number of iterations of each particle and the predicted starting point T.

The final RUL prediction results and their distribution histograms, which are statistical analysis of the lifetime values of all particles, are shown in Fig. 6.

The RUL prediction results and their distribution histograms at the starting point of Battery005, that is, $T = 80$, are shown in Fig. 7. And the RUL prediction of Battery006 and Battery018 are also drawn in Figs. 8 and 9 respectively.

In order to evaluate the accuracy of the prediction results simply, an equation for predicting error that is the difference between the actual RUL value and the predicted RUL value is defined as shown in the following.

$$RUL_e = RUL_t - RUL_p \tag{17}$$

where RUL_t represents the actual number of remaining useful life cycles, and RUL_p represents the predicted number of remaining useful life cycles predicted by the algorithm in the paper.

According to the above definition, as shown in Fig. 7, it can be seen that the actual end of life cycle of the Battery005 is 126, and the average life cycle number predicted by the method proposed in this paper is 138. When the prediction starting point is set to $T = 80$, the actual remaining life is $RUL_t = 46$ and the predicted remaining life is $RUL_p = 58$, so the prediction error of the algorithm $RUL_e = RUL_p$-$RUL_t = 12$. When the prediction starting point is set to $T = 60$ and $T = 100$ respectively, the prediction error of

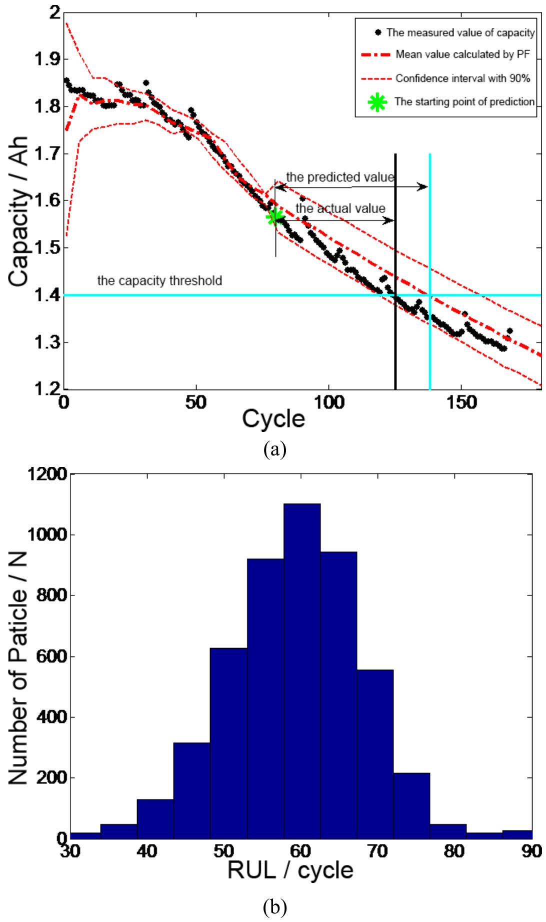

FIGURE 7. The RUL prediction results of Battery005 at the starting point $T = 80$. (a) The capacity degeneration curve. (b) The RUL distribution histogram.

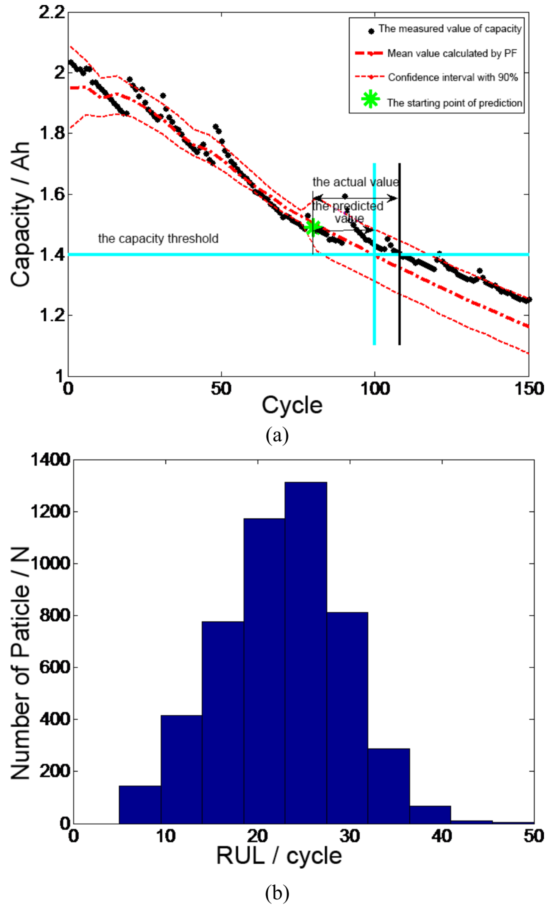

FIGURE 8. The RUL prediction results of Battery006 at the starting point $T = 80$. (a) The capacity degeneration curve. (b) The RUL distribution histogram.

TABLE 1. The RUL prediction error of Battery005 at the different starting point.

Battery ID	Starting point	Actual life/Actual remaining life	Predicted life/Predicted remaining life	RUL prediction error
Battery005	60	126/66	155/95	29
Battery005	80	126/46	138/58	12
Battery005	100	126/26	134/34	8

the algorithm is also obtained. Table 1 shows the prediction error of the Battery005 at different prediction starting points.

C. RUL PREDICTION RESULTS OF DIFFERENT CONDITIONS ON FORECAST STARTING POINTS

The Battery018 experiment chooses the number of cycles in the early, middle and end of life as the starting point, that is, the prediction starting points are $T = 40$, $T = 60$ and $T = 80$ respectively. Algorithms according to the process steps mentioned above are performed prediction process and the learning process, and the average capacity degradation curves were obtained and compared with the actual end of the life. According to the prediction model based on the exponential model and the PF, Battery018 is predicted and the capacity degradation path and curve at different starting points is shown in Fig. 10. In the Battery006 experiment, the prediction starting points T are 60, 80 and 100 respectively, and the capacity degradation path and curve at different starting points is shown in Fig. 11.

The RUL predictive error quantification of three batteries at different prediction starting point was shown in Table 2. For Battery005, when the starting point for prediction T is set as 60, 80 and 100 respectively, the predicted average life expectancy termination points are 155, 138 and 134 respectively, which are gradually close to its actual life of 126. The same is for Battery006 and Battery018. In Table 2, from the overall trends reflected by these three batteries, it can be seen that as the prediction starting point continues to be pushed back, the prediction error becomes closer to zero, which is in good agreement with the actual application. It also shows that the algorithm has convergence. With the pushback of the starting point for prediction, more and more capacity data can be used for learning, and more rich degradation information

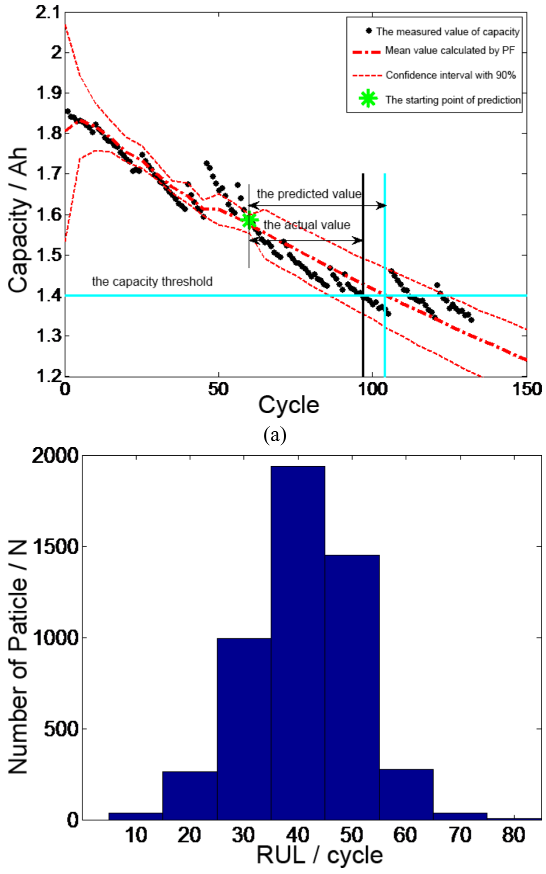

(a)

(b)

FIGURE 9. **The RUL prediction results of Battery018 at the starting point $T = 60$. (a) The capacity degeneration curve. (b) The RUL distribution histogram.**

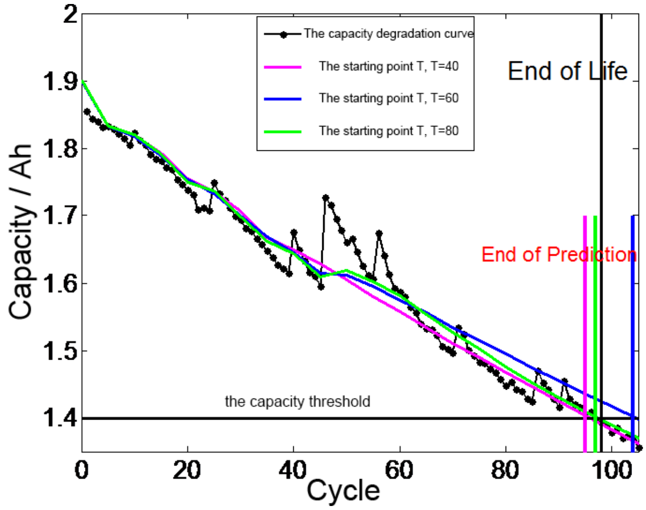

FIGURE 10. **The RUL prediction results of Battery018 at the different starting point.**

and features are contained. Therefore, the prediction error is smaller in the backward direction.

It can be seen from many examples in this section that the residual life prediction method based on the PF requires less prior information for individuals and is therefore more convenient to implement. The algorithm can adapt to the degradation difference between different samples, and at the same time it gives a relatively accurate residual life prediction value of individual battery capacity degradation, more and more prediction data are available with the passage of time, and the prediction error also gradually decreases. And the algorithm can realize the indefinite expression of the prediction result. Compared with the point estimation, the interval estimation of the probability density has a greater reference value for the maintenance strategy because the uncertainty factor always exists, and the probability density function is a good solution.

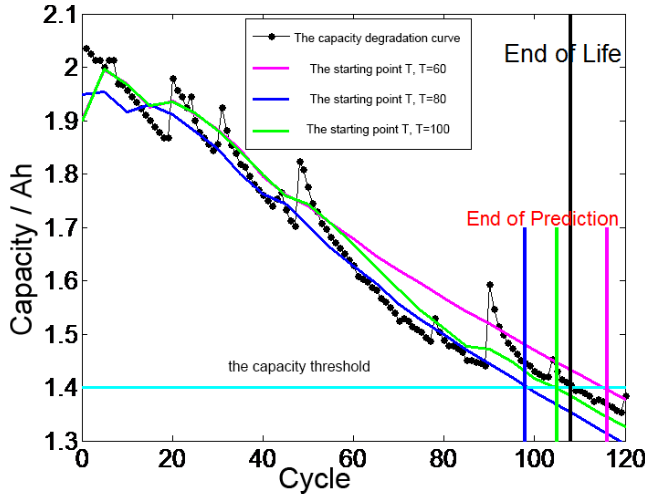

FIGURE 11. **The RUL prediction results of Battery006 at the different starting point.**

TABLE 2. **The contrast of the RUL prediction error of LIBs at the different starting point.**

Battery ID	Starting point	Actual life	Predicted life	RUL prediction error
	60		155	29
Battery005	80	126	138	12
	100		134	8
	60		117	9
Battery006	80	108	98	-10
	100		105	-3
	40		95	-3
Battery018	60	98	104	6
	80		97	-1

The RUL prediction errors calculated by the autoregressive integrated moving average (ARIMA) prediction algorithm in [36] and the fusion nonlinear degradation autoregressive model and the regularized particle filter (AR-RPF) prediction algorithm in [26] are shown in Table 3. From the

TABLE 3. **The comparision of the RUL prediction error of LIBs.**

Algorithm	Battery ID	Starting point	Actual remaining life	Predicted remaining life	RUL prediction error
ARIMA	Battery 005	60	66	53	-13
		80	46	29	-17
		100	26	18	-8
	Battery 006	50	58	75	17
		60	48	34	-14
		80	28	13	-15
AR-RPF	Battery 005	60	66	50	16
		80	46	40	6
		100	26	32	6
	Battery 006	60	48	44	-4
		80	28	36	8
		100	8	12	4

error of prediction results, the prediction method based on the exponential model and the PF proposed in this paper has better prediction accuracy and good convergence than other prediction methods.

V. RESULTS AND DISCUSSION

The algorithm proposed in this paper will be evaluated according to the general evaluation index proposed by the relevant scholars, and the quantitative representation of the histogram will be quantified.

A. PREDICTION ALGORITHM PERFORMANCE EVALUATION INDEX

In this paper two performance evaluation indictors, the prognostic horizon and the precision index, are presented for the prediction algorithm.

1) PROGNOSTIC HORIZON (PH) INDEX

First, when we evaluate a prediction algorithm, the prognostic horizon can be defined as the time between the indices of the time i and the end of life interval when the prediction error of the algorithm satisfies the pre-given prediction error requirement for the first time, as following equation.

$$PH = EOL - i \tag{18}$$

According to the above description of the PH index, as shown in Figs. 12 and 13, PH results with 10% error margin of Battery006 and Battery018 were 58, 38 respectively. It can be seen from Fig. 13 that the PH index does not guarantee that the subsequent prediction error is within a given error range. For example, the Battery018 meets the requirement of 10% error at $T = 40$ at the first time, but the prediction error is greater than the given error range of 10% when $T = 60$. It can be found that the PH index does not guide significance to the convergence of the prediction algorithm. Therefore, more demanding indexes are needed to evaluate the prediction performance of the prediction algorithm.

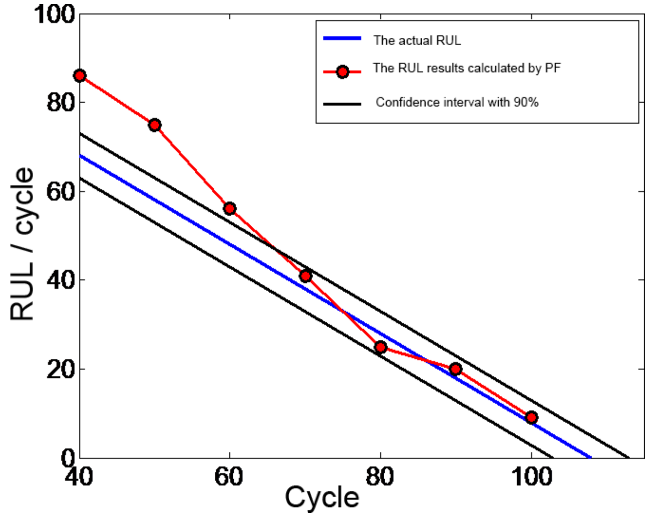

FIGURE 12. **The RUL prediction results of PH with 10% error margin of Battery006.**

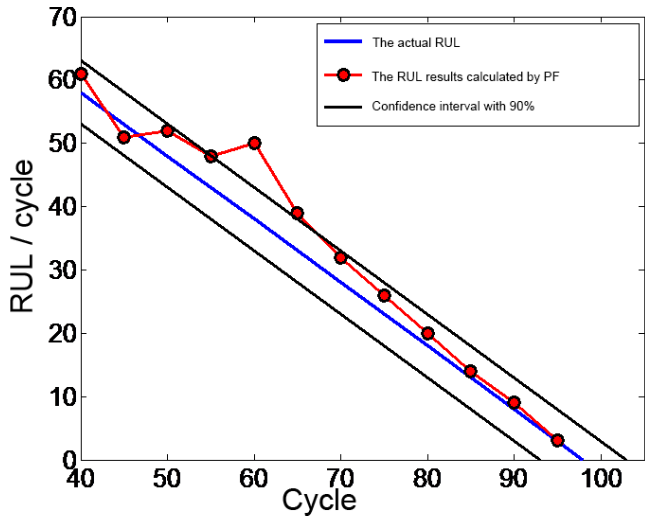

FIGURE 13. **The RUL prediction results of PH with 10% error margin of Battery018.**

2) PRECISION INDEX ($\alpha - \lambda$)

The PH index cannot evaluate the prediction algorithm, and the weak point leads to a new indicator: $\alpha - \lambda$ accuracy, which denotes that the prediction algorithm reaches a specified error level or accuracy over a specified time period, and can be defined as following:

$$(1-\alpha)r(t) \leq r(t_\lambda) \leq (1+\alpha)r(t) \tag{19}$$

where α indicates a predetermined error accuracy, and λ indicates a time window.

According to the above definition, the different starting point prediction results and $\alpha - \lambda$ accuracy of Battery006 and Battery018 shown in Figs. 14 and 15 respectively. It can be seen from the figures that the accuracy of the prediction algorithm is more stringent than that of the PH index, and its prediction accuracy is more stringent with the passage of

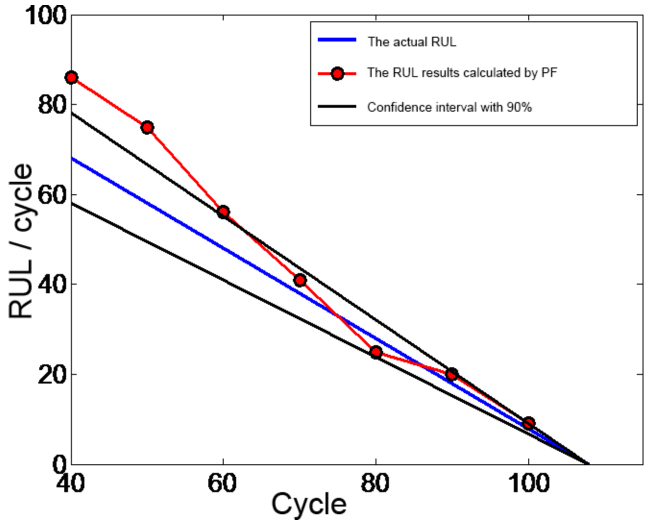

FIGURE 14. The RUL prediction results of $\alpha - \lambda$ accurate indicators of Battery006.

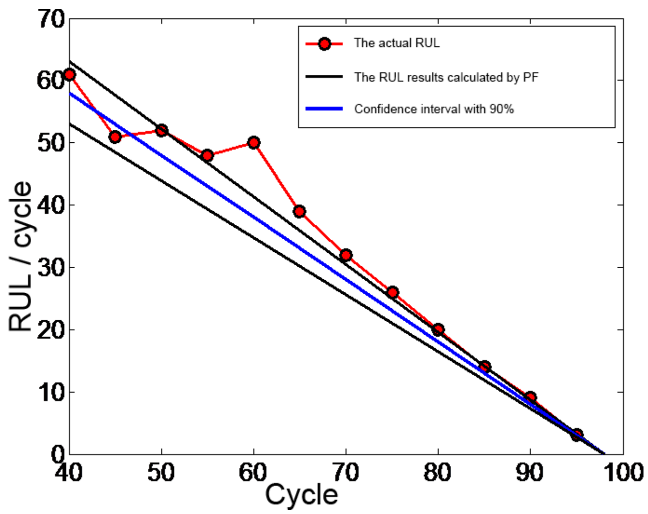

FIGURE 15. The RUL prediction results of $\alpha - \lambda$ accurate indicators of Battery018.

time, which is also consistent with the actual requirement, because at the period of end the more precise prediction error, the higher prediction accuracy requirements. It can be seen that Battery006 satisfies the given $\alpha - \lambda$ accuracy requirement after $T = 60$, and Battery018 satisfies the given $\alpha - \lambda$ accuracy requirement after $T = 80$, so the former is better than the latter.

B. THE PREDICTION RESULTS OF UNCERTAINTIES

In the engineering practice, engineers are not likely to use a distribution histogram as a basis for making a maintenance decision. In order to give the maintenance decision-making scientific basis, this section expresses the RUL histogram, and gives an uncertainty quantification expression.

1) CONFIDENCE INTERVAL

The confidence interval is the statistical evaluation index, and the specific definition is as follows: given a general parameter θ for an overall and two parameters θ_L, θ_U for two samples, the formula (θ_L, θ_U) denotes the confidence interval with parameter θ and confidence $1 - \alpha$ if a formula is established as follows for some significant level $\alpha(0 < \alpha < 1)$:

$$P(\theta_L \leq \alpha \leq \theta_U) = 1 - \alpha \tag{20}$$

For the standard Normal distribution, according to the significant level the confidence interval can be obtained by simple empirical formula calculation.

When we use the Monte Carlo method to obtain a parameter value estimation of distribution, the confidence interval calculation steps are as follows: first of all, the samples for all parameters are sorted in ascending order according to the size of their estimated value.

When the significant level is set to $\alpha = 0.1$, the upper limit θ_U of the confidence interval is equal to that value where is located at 95% position after sorting, and the corresponding lower limit θ_L of the confidence interval is equal to that value where is located at 5% position after sorting. Similarly, when the significant level is set to $\alpha = 0.05$ and $\alpha = 0.01$ respectively, the upper limit θ_U is equal to that value where is located at 97.5% and 99.5% position respectively after sorting, and the lower limit θ_L is equal to that value where is located at 2.5% and 0.5% respectively after sorting.

According to the sorting method, the confidence intervals for the prediction of the RUL can be calculated, and the histogram distribution diagram based on PF is shown in Fig. 16.

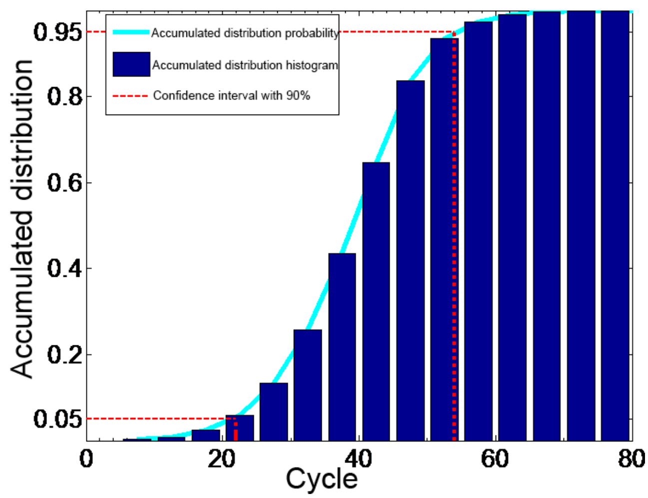

FIGURE 16. The RUL prediction results with confidence interval 90%.

It can be seen from the figure that the confidence interval $(\theta_L, \theta_U) = (22, 54)$, when a confidence level is equal to $1-\alpha = 90\%$, namely the RUL of LIBs has a 90% probability of falling in the interval.

2) DISTRIBUTION HYPOTHESIS TEST

The K-S test is a method of statistics that is commonly used to analyze a set of data distribution, and its basic idea is to calculate the cumulative distribution function through a set of data for testing and to compare with a standard distribution, and it accepts the test or rejects the hypothesis under a given confidence level.

Therefore, the life distribution of the histogram will also use the K-S test by the prediction test. Through the K-S test in MATLAB, it is found that the Battery018 prediction results of the probability distribution histogram conform to the Weibull distribution under the 90% confidence level. According to the Weibull density function fitting prediction of life distribution histogram, the fitting effect with the original histogram is shown in Fig. 17.

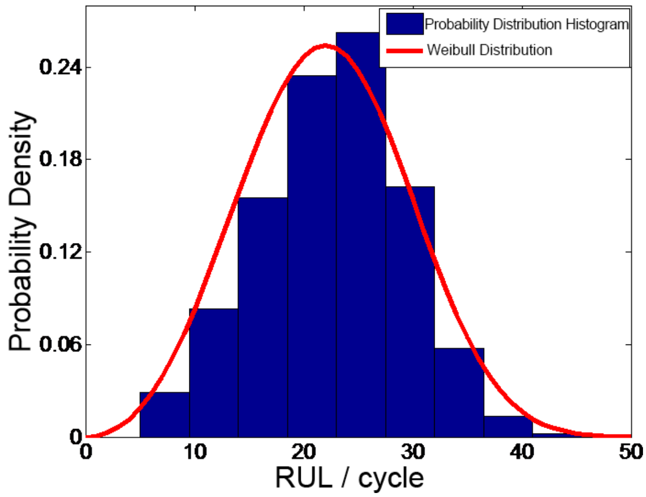

FIGURE 17. **The distribution histogram of RUL prediction results and Weibull distribution.**

The Weibull distribution accords with the life distribution of the most mechanics parts, and it verifies that the proposed prediction algorithm is reasonable and effective. We also study the Normal distribution and other common Poisson distribution, and it does not comply with these common under the same 90% confidence level.

VI. CONCLUSION

In this paper, the algorithm framework based on the exponential model and the PF for predicting the remaining life of LIBs is proposed. And the NASA PCoE battery test data are analyzed with a large number of cases. Each case is given to predict average degradation path and the final life probability distribution histogram. The prediction results show that the proposed prediction algorithm has quite good forecast effect. The main research achievements are as following.

(1) The PF algorithm based on the framework for predicting the remaining life prediction of LIBs was established. Combined with a large number of cases, it gives the prediction error under the condition of different prediction. Compared with other papers in the ARIMA prediction algorithm and the AR-RPF algorithm, the results show that the proposed algorithm has a better prediction performance. The results show that the proposed algorithm has a better prediction performance.

(2) The use of the PH index and the $\alpha - \lambda$ precision index are used to evaluate the prediction performance of the proposed algorithm. Sometimes, The PH index cannot evaluate the prediction algorithm, and the $\alpha - \lambda$ precision index denotes the specified error level or accuracy successfully. From the calculation results of these indicators, this exponential model and the prediction method have better prediction accuracy and convergence.

(3) According to the prediction residual life distribution histogram, confidence intervals are calculated and examined on the Weibull distribution assumption. From the experiments, the prediction results of probability distribution histogram conform to the Weibull distribution under the 90% confidence level. The prediction result of post-processing is more conducive to the maintenance personnel for optimizing the maintenance strategy.

ACKNOWLEDGMENT

We thank PCoE in NASA for sharing benchmark data of lithium-ion batteries.

REFERENCES

[1] M. A. Hannan, M. M. Hoque, A. Mohamed, and A. Ayob, "Review of energy storage systems for electric vehicle applications: Issues and challenges," *Renew. Sustain. Energy Rev.*, vol. 69, pp. 771–789, Mar. 2017.

[2] X. Hu, C. Zou, C. Zhang, and Y. Li, "Technological developments in batteries: A survey of principal roles, types, and management needs," *IEEE Power Energy Mag.*, vol. 15, no. 5, pp. 20–31, Sep. 2017.

[3] M. Berecibar, I. Gandiaga, I. Villarreal, N. Omar, J. Van Mierlo, and P. Van den Bossche, "Critical review of state of health estimation methods of Li-ion batteries for real applications," *Renew. Sustain. Energy Rev.*, vol. 56, pp. 572–587, Apr. 2016.

[4] B. Scrosati and J. Garche, "Lithium batteries: Status, prospects and future," *J. Power Sources*, vol. 195, no. 9, pp. 2419–2430, May 2010.

[5] G. K. Prasad and C. D. Rahn, "Model based identification of aging parameters in lithium-ion batteries," *J. Power Sources*, vol. 232, pp. 79–85, Jun. 2013.

[6] E. Walker, S. Rayman, and R. E. White, "Comparison of a particle filter and other state estimation methods for prognostics of lithium-ion batteries," *J. Power Sources*, vol. 287, pp. 1–12, Aug. 2015.

[7] S. S. Y. Ng, Y. Xing, and K. L. Tsui, "A naive Bayes model for robust remaining useful life prediction of lithium-ion battery," *Appl. Energy*, vol. 118, pp. 114–123, Apr. 2014.

[8] X. S. Si, W. Wang, C. H. Hu, and D.-H. Zhou, "Remaining useful life estimation—A review on the statistical data driven approaches," *Eur. J. Oper. Res.*, vol. 213, no. 1, pp. 1–14, Aug. 2011.

[9] W. Waag, C. Fleischer, and D. U. Sauer, "Critical review of the methods for monitoring of lithium-ion batteries in electric and hybrid vehicles," *J. Power Sources*, vol. 258, pp. 321–339, Jul. 2014.

[10] L. Lu, X. Han, J. Li, J. Hua, and M. Ouyang, "A review on the key issues for lithium-ion battery management in electric vehicles," *J. Power Sources*, vol. 226, pp. 272–288, Mar. 2013.

[11] D. Wang, Q. Miao, and M. Pecht, "Prognostics of lithium-ion batteries based on relevance vectors and a conditional three-parameter capacity degradation model," *J. Power Sources*, vol. 239, pp. 253–264, Oct. 2013.

[12] A. Eddahech, O. Briat, E. Woirgard, and J. M. Vinassa, "Remaining useful life prediction of lithium batteries in calendar ageing for automotive applications," *Microelectron. Rel.*, vol. 52, no. 9, pp. 2438–2442, Sep. 2012.

[13] C. Zhang, Y. He, L. Yuan, and S. Xiang, "Capacity prognostics of lithium-ion batteries using EMD denoising and multiple kernel RVM," *IEEE Access*, vol. 5, pp. 12061–12070, Jun. 2017.

[14] D. Andre, A. Nuhic, T. Soczka-Guth, and D. U. Sauer, "Comparative study of a structured neural network and an extended Kalman filter for state of health determination of lithium-ion batteries in hybrid electric vehicles," *Eng. Appl. Artif. Intell.*, vol. 26, no. 3, pp. 951–961, Mar. 2013.
[15] D. Liu, H. Wang, Y. Peng, W. Xie, and H. Liao, "Satellite lithium-ion remaining cycle life prediction with novel indirect health indicator extraction," *Energies*, vol. 6, no. 8, pp. 3654–3668, Jul. 2013.
[16] Y.-J. He, J.-N. Shen, J.-F. Shen, and Z.-F. Ma, "State of health estimation of lithium-ion batteries: A multiscale Gaussian process regression modeling approach," *AIChE J.*, vol. 61, no. 5, pp. 1589–1600, Mar. 2015.
[17] B. Long, W. Xian, L. Jiang, and Z. Liu, "An improved autoregressive model by particle swarm optimization for prognostics of lithium-ion batteries," *Microelectron. Rel.*, vol. 53, no. 6, pp. 821–831, 2013.
[18] Y. Zhou and M. Huang, "Lithium-ion batteries remaining useful life prediction based on a mixture of empirical mode decomposition and ARIMA model," *Microelectron. Rel.*, vol. 65, pp. 265–273, Oct. 2016.
[19] C. Weng, Y. Cui, J. Sun, and H. Peng, "On-board state of health monitoring of lithium-ion batteries using incremental capacity analysis with support vector regression," *J. Power Sources*, vol. 235, pp. 36–44, Aug. 2013.
[20] H. Dong, X. Jin, Y. Lou, and C. Wang, "Lithium-ion battery state of health monitoring and remaining useful life prediction based on support vector regression-particle filter," *J. Power Sources*, vol. 271, pp. 114–123, Aug. 2014.
[21] D. Liu, J. Zhou, D. Pan, Y. Peng, and X. Peng, "Lithium-ion battery remaining useful life estimation with an optimized relevance vector machine algorithm with incremental learning," *Measurement*, vol. 63, pp. 143–151, Mar. 2015.
[22] S. Peng, C. Chen, H. Shi, and Z. Yao, "State of charge estimation of battery energy storage systems based on adaptive unscented Kalman filter with a noise statistics estimator," *IEEE Access*, vol. 5, pp. 13202–13212, Jul. 2017.
[23] F. Li and J. Xu, "A new prognostics method for state of health estimation of lithium-ion batteries based on a mixture of Gaussian process models and particle filter," *Microelectron. Rel.*, vol. 55, no. 7, pp. 1035–1045, Jun. 2015.
[24] C. Zou, C. Manzie, D. Nešić, and A. G. Kallapur, "Multi-time-scale observer design for state-of-charge and state-of-health of a lithium-ion battery," *J. Power Sources*, vol. 335, pp. 121–130, Dec. 2016.
[25] C. Zou, X. Hu, Z. Wei, and X. Tang, "Electrothermal dynamics-conscious lithium-ion battery cell-level charging management via state-monitored predictive control," *Energy*, vol. 141, pp. 250–259, Dec. 2017.
[26] D. Liu, Y. Luo, J. Liu, Y. Peng, L. Guo, and M. Pecht, "Lithium-ion battery remaining useful life estimation based on fusion nonlinear degradation AR model and RPF algorithm," *Neural Comput. Appl.*, vol. 25, nos. 3–4, pp. 557–572, Sep. 2014.
[27] Y. Hu, P. Baraldi, F. D. Maio, and E. Zio, "A particle filtering and kernel smoothing-based approach for new design component prognostics," *Rel. Eng. Syst. Safety*, vol. 134, pp. 19–31, Feb. 2015.
[28] Q. Miao, L. Xie, H. Cui, W. Liang, and M. Pecht, "Remaining useful life prediction of lithium-ion battery with unscented particle filter technique," *Microelectron. Rel.*, vol. 53, pp. 805–810, Jun. 2013.
[29] D. Wang, F. Yang, K.-L. Tsui, Q. Zhou, and S. J. Bae, "Remaining useful life prediction of lithium-ion batteries based on spherical cubature particle filter," *IEEE Trans. Instrum. Meas.*, vol. 65, no. 6, pp. 1282–1291, Jun. 2016.
[30] X. Zhang, Q. Miao, and Z. Liu, "Remaining useful life prediction of lithium-ion battery using an improved UPF method based on MCMC," *Microelectron. Rel.*, vol. 75, pp. 288–295, Aug. 2017.
[31] Y. Xing, E. W. M. Ma, K.-L. Tsui, and M. Pecht, "An ensemble model for predicting the remaining useful performance of lithium-ion batteries," *Microelectron. Rel.*, vol. 53, no. 6, pp. 811–820, Jun. 2013.
[32] F. Yang, D. Wang, Y. Xing, and K.-L. Tsui, "Prognostics of $Li(NiMnCo)O_2$-based lithium-ion batteries using a novel battery degradation model," *Microelectron. Rel.*, vol. 70, pp. 70–78, Mar. 2017.
[33] Z. Wang, J. Ma, and L. Zhang, "State-of-health estimation for lithium-ion batteries based on the multi-Island genetic algorithm and the Gaussian process regression," *IEEE Access*, vol. 5, pp. 21286–21295, 2017.
[34] F. Gustafsson, "Particle filter theory and practice with positioning applications," *IEEE Aerosp. Electron. Syst. Mag.*, vol. 25, no. 7, pp. 53–82, Jul. 2010.
[35] M. S. Arulampalam, S. Maskell, N. Gordon, and T. Clapp, "A tutorial on particle filters for online nonlinear/non-Gaussian Bayesian tracking," *IEEE Trans. Signal Process.*, vol. 50, no. 2, pp. 174–188, Feb. 2002.
[36] M. Jouin, R. Gouriveau, D. Hissel, M.-C. Péra, and N. Zerhouni, "Particle filter-based prognostics: Review, discussion and perspectives," *Mech. Syst. Signal Process.*, vols. 72–73, pp. 2–31, May 2016.
[37] X. H. Su, S. Wang, M. Pecht, L. L. Zhao, and Z. Ye, "Interacting multiple model particle filter for prognostics of lithium-ion batteries," *Microelectron. Rel.*, vol. 70, pp. 59–69, Mar. 2017.
[38] B. Saha and K. Goebel, "Battery data set," NASA Ames Prognostics Data Repository, NASA Ames Res., Center, Moffett Field, CA, USA, 2007. [Online]. Available: http://ti.arc.nasa.gov/project/prognostic-data-repository

LIJUN ZHANG was born in Beipiao, Liaoning, China, in 1978. He received the B.S., M.S., and Ph.D. degrees in mechanical engineering from the University of Science and Technology Beijing.

Since 2009, he has been an Associate Professor with the National Center for Materials Service Safety. He has authored over 30 articles and two books. His research interests include prognostics and health management for lithium-ion batteries and mechanical equipments.

Dr. Zhang has been a Committee Member for Equipment and Maintenance Engineering Branch, China Mechanical Engineering Society, since 2016.

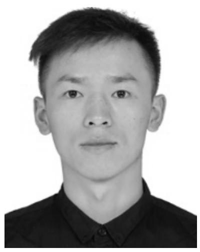

ZHONGQIANG MU was born in Zheng'an, Guizhou, China, in 1992. He received the B.A. degree in mechanical engineering from the University of Science and Technology Beijing (USTB), in 2016, where he is currently pursuing the master's degree.

His main research interests are in the areas of prognostics and health management for lithium-ion batteries.

CHANGYAN SUN was born in Jingzhou, Hubei, China, in 1979. She received the B.S., M.S., and Ph.D. degrees in inorganic chemistry from Beijing Normal University.

From 2008 to 2016, she was an Associate Professor with the School of Chemistry and Biological Engineering, University of Science and Technology Beijing (USTB). Since 2017, she has been a Professor with the Chemistry and Chemical Engineering Department, USTB. She has authored over 60 articles and one book. Her research interests include lithium-ion batteries, optoelectronic functional materials, and fluorescent probes.

Dr. Sun was a recipient of Beijing Higher Education Young Elite Teacher Project in 2013.